Dicopper(I) Complexes with Reduced States of 3,6-Bis(2′-pyrimidyl)-1,2,4,5-tetrazine: Crystal Structures and Spectroscopic Properties of the Free Ligand, a Radical Species, and a Complex of the 1,4-Dihydro Form

Markus Glöckle,[†] Klaus Hübler,[†] Hans-Jürgen Kümmerer,[‡] Gert Denninger,[‡] and Wolfgang Kaim*,[†]

Institut für Anorganische Chemie, Universität Stuttgart, Pfaffenwaldring 55, D-70550 Stuttgart, Germany, and Physikalisches Institut, Universität Stuttgart, Pfaffenwaldring 57, D-70550 Stuttgart, Germany

Received November 6, 2000

The complexes $\{(\mu\text{-bmtz}^{\bullet-})[Cu(PPh_3)_2]_2\}(BF_4)$ (**1**) and $\{(\mu\text{-}H_2\text{bmtz})[Cu(PPh_3)_2]_2\}(BF_4)_2$ (**2**) (bmtz = 3,6-bis(2′-pyrimidyl)-1,2,4,5-tetrazine and H_2bmtz = 1,4-dihydro-3,6-bis(2′-pyrimidyl)-1,2,4,5-tetrazine) were obtained as stable materials that could be crystallized for structure determination. **1**·2 CH_2Cl_2: $C_{84}H_{70}BCl_4Cu_2F_4N_8P_4$; monoclinic, $C2/c$; a = 26.215(7) Å, b = 22.122(6) Å, c = 18.114(5) Å, β = 133.51(1)°; Z = 4. **2**·CH_2Cl_2: $C_{83}H_{70}B_2Cl_2Cu_2F_8N_8P_4$; triclinic, $P\bar{1}$; a = 10.948(2) Å, b = 12.067(2) Å, c = 30.287(6) Å, α = 93.82(3)°, β = 94.46(3)°, γ = 101.60(3)°; Z = 2. Bmtz itself was also structurally characterized ($C_{10}H_6N_8$; monoclinic, $P2_1/c$; a = 3.8234(8) Å, b = 10.147(2) Å, c = 13.195(3) Å, β = 94.92(3)°; Z = 2). Whereas the radical complex ion contains a planar tetrazine ring in the center, the 1,4-dihydrotetrazine heterocycle in the corresponding complex of H_2bmtz is considerably folded. Both systems exhibit slight twists between the tetrazine and the pyrimidine rings. The intra-tetrazine distances are characteristically affected by the electron transfer, as is also evident from a comparison with the new structure of free bmtz; the bonding to copper(I) changes accordingly. Spectroscopy including X- and W-band EPR of the radical species confirms that the electron addition is mainly to the tetrazine ring.

Introduction

Coordination compounds between copper(I) as a structurally flexible template center and multifunctional organic ligands have been used to construct a large variety of unusual structures in supramolecular chemistry.[1,2] Examples include catenates[3] and molecular knots,[4] grids,[5] helicates,[6] and decks.[7] To extend this scope, we have recently presented the new potentially tetrakis-bischelate ligand 3,6-bis(2′-pyrimidyl)-1,2,4,5-tetrazine (bmtz)[8] and described its capacity for inducing strong metal−metal interaction in dinuclear $Fe^{II}Fe^{III}$ or $Ru^{II}Ru^{III}$ mixed-valent situations.[8,9]

As a highly electron-deficient and multiply nucleophilic molecule, bmtz can be expected, like 1,2,4,5-tetrazines in general,[10] to undergo stepwise reduction and protonation, leading to 1,4-dihydro derivatives[11] after a $2e/2H^+$ process. Yet, the ability of bmtz to bind metal centers via the azo-imine chelating groups should remain because there are four such moieties in bmtz with only two being engaged in the reductive protonation. Thus, bmtz is a multifunctional system where coupling of electron and proton transfer *and* interaction with two metal centers can occur.

The bmtz ligand is related to 3,6-bis(2′-pyridyl)-1,2,4,5-tetrazine (bptz);[12] bptz and the isomeric 3,6-bis(4′-pyridyl)-1,2,4,5-tetrazine[13] have been used as strong acceptor ligands[12−21] and, more recently, as components of supramolecular structures.[22−24] Nitrogen-rich unsaturated ligands such as bptz[25−28]

[†] Institut für Anorganische Chemie.
[‡] Physikalisches Institut.

(1) Munakata, M.; Wu, L. P.; Kuroda-Sowa, T. *Adv. Inorg. Chem.* **1999**, *46*, 173.
(2) Swiegers, G. T.; Malefetse, T. J. *Chem. Rev.* **2000**, *100*, 3483.
(3) (a) Livoreil, A.; Dietrich-Buchecker, C.; Sauvage, J.-P. *J. Am. Chem. Soc.* **1994**, *116*, 9399. (b) Baumann, F.; Livoreil, A.; Kaim, W.; Sauvage, J.-P. *J. Chem. Soc., Chem. Commun.* **1997**, 35.
(4) Chambron, J.-C.; Dietrich-Buchecker, C. O.; Nierengarten, J.-F.; Sauvage, J.-P.; Solladié, N.; Albrecht-Gary, A. M.; Meyer, M. *New J. Chem.* **1995**, *19*, 409.
(5) (a) Baxter, P. N. W.; Lehn, J.-M.; Fischer, J.; Yoinou, M.-T. *Angew. Chem.* **1994**, *106*, 2432; *Angew. Chem., Int. Ed. Engl.* **1994**, *33*, 2284. (b) Bassani, D. M.; Lehn, J.-M.; Fromm, K.; Fenske, D. *Angew. Chem.* **1998**, *110*, 2534; *Angew. Chem., Int. Ed. Engl.* **1998**, *37*, 2364.
(6) Hasenknopf, B.; Lehn, J.-M.; Boumediene, N.; Dupont-Gervais, A.; Van Dorsselaer, A.; Kneisel, B.; Fenske, D. *J. Am. Chem. Soc.* **1997**, *119*, 10956.
(7) Schwach, M.; Hausen, H.-D.; Kaim, W. *Chem.—Eur. J.* **1996**, *2*, 446.
(8) Kaim, W.; Fees, J. *Z. Naturforsch.* **1995**, *50b*, 123.
(9) Ketterle, M.; Fiedler, J.; Kaim, W. *J. Chem. Soc., Chem. Commun.* **1998**, 1701.
(10) Neugebauer, F. A.; Krieger, C.; Fischer, H.; Siegel, R. *Chem. Ber.* **1983**, *116*, 2261.
(11) Hausen, H.-D.; Hornung, F.-M.; Ketterle, M.; Schwach, M.; Kaim, W. Unpublished results.
(12) Kohlmann, S.; Ernst, S.; Kaim, W. *Angew. Chem.* **1985**, *97*, 698; *Angew. Chem., Int. Ed. Engl.* **1985**, *24*, 684.
(13) Kaim, W.; Kohlmann, S. *Inorg. Chem.* **1990**, *29*, 1898.
(14) Kaim, W.; Kohlmann, S. *Inorg. Chem.* **1987**, *26*, 68.
(15) Kaim, W.; Kohlmann, S. *Inorg. Chem.* **1987**, *26*, 1469.
(16) Ernst, S. D.; Kaim, W. *Inorg. Chem.* **1989**, *28*, 1520.
(17) Kaim, W.; Kohlmann, S. *Inorg. Chem.* **1990**, *29*, 2909.
(18) Klein, A.; Hasenzahl, S.; Kaim, W.; Fiedler, J. *Organometallics* **1998**, *17*, 3532.
(19) Poppe, J.; Moscherosch, M.; Kaim, W. *Inorg. Chem.* **1993**, *32*, 2640.
(20) Roche, S.; Thomas, J. A.; Yellowlees, L. J. *J. Chem. Soc., Chem. Commun.* **1998**, 1429.
(21) Glöckle, M.; Fiedler, J.; Katz, N. E.; Garcia Posse, M.; Cutin, E.; Kaim, W. *Inorg. Chem.* **1999**, *38*, 3270.
(22) Campos-Fernández, C. S.; Clérac, R.; Dunbar, K. R. *Angew. Chem.* **1999**, *111*, 3685; *Angew. Chem., Int. Ed.* **1999**, *38*, 3477.
(23) Withersby, M. A.; Blake, A. J.; Champness, N. R.; Cooke, P. A.; Hubberstey, P.; Schöder, M. *J. Am. Chem. Soc.* **2000**, *122*, 4044.

10.1021/ic001228q CCC: $20.00
Published on Web 04/06/2001

Table 1. Crystallographic and Refinement Data

	bmtz	**1**·2CH_2Cl_2	**2**·CH_2Cl_2
empirical formula	$C_{10}H_6N_8$	$C_{84}H_{70}BCl_4Cu_2F_4N_8P_4$	$C_{83}H_{70}B_2Cl_2Cu_2F_8N_8P_4$
fw	238.23	1671.05	1674.95
temp (K)	173(2)	173(2)	173(2)
wavelength (Å)	0.710 73	0.710 73	0.710 73
cryst syst	monoclinic	monoclinic	triclinic
space group	$P2_1/c$ (No. 14)	$C2/c$ (No. 15)	$P\bar{1}$ (No. 2)
a (Å)	3.8234(8)	26.215(7)	10.948(2)
b (Å)	10.147(2)	22.122(6)	12.067(2)
c (Å)	13.195(3)	18.114(5)	30.287(6)
α (deg)	90	90	93.82(3)
β (deg)	94.92(3)	133.51(1)	94.46(3)
γ (deg)	90	90	101.60(3)
V (Å^3)	510.1(2)	7619(3)	3893.8(14)
Z	2	4	2
ρ_{calcd} (g cm^{-3})	1.551	1.457	1.429
μ (mm^{-1})	0.108	0.845	0.767
GOF	1.052	1.008	1.196
final R indices [$I > 2\sigma(I)$] (all data)[a]	$R_1 = 0.0426$ $R_w = 0.1334$	$R_1 = 0.0763$ $R_w = 0.2168$	$R_1 = 0.0763$ $R_w = 0.1952$

[a] $R_1 = (\sum||F_o| - |F_c||)/\sum|F_o|$. $R_w = \{\sum[w(|F_o|^2 - |F_c|^2)^2]/\sum[w(F_o^2)^2]\}^{1/2}$.

and the recently described 2,2′-azobis(5-chloropyrimidine)[29] are known to form radical complexes rather easily.

In this report we describe the crystal structure of bmtz as well as structural and spectroscopic studies of two dicopper(I) complexes of the reduced forms of bmtz, viz., the radical ion complex {(μ-bmtz$^{\bullet-}$)[Cu(PPh_3)$_2$]$_2$}(BF_4) (**1**) and the corresponding 1,4-dihydro species {(μ-H_2bmtz)[Cu(PPh_3)$_2$]$_2$}(BF_4)$_2$ (**2**) (H_2bmtz = 1,4-dihydro-3,6-bis(2′-pyrimidyl)-1,2,4,5-tetrazine). The crystallographic results thus allowed us to structurally compare compounds of all three components within the redox system bmtz$^{0/\bullet-/2-}$. In addition to the structural information, spectroscopic data were obtained to assess the electronic structures of the compounds.

Experimental Section

Instrumentation. X-band EPR spectra at about 9.5 GHz were recorded on a Bruker System ESP 300 equipped with a Bruker ER035M gaussmeter and a HP 5350B microwave counter. W-band EPR spectra at about 94 GHz were obtained with a Bruker ELEX SYS E680 spectrometer. ^{1}H NMR spectra were taken on a Bruker AC 250 spectrometer. UV/vis absorption spectra were recorded on a Bruins Instruments Omega 10 spectrophotometer. Cyclic voltammetry was carried out at 50 mV/s standard scan rate in dichloromethane/0.2 M Bu_4NPF_6 at 203 K, using a three-electrode configuration (glassy carbon or Pt working electrode, Pt counter electrode, Ag/AgCl reference) and a PAR 273 potentiostat and function generator. The ferrocene/ferrocenium couple served as the internal reference.

{(μ-bmtz)[Cu(PPh_3)$_2$]$_2$}(BF_4) (1). A mixture containing 72.4 mg (0.304 mmol) of bmtz,[8] 159.3 mg (0.607 mmol) of PPh_3, and 19.4 mg (0.305 mmol) of activated copper powder in 15 mL of dried dichloromethane was stirred for 1 day at room temperature. (Activation of Cu was accomplished by washing with hydrochloric acid, degassed water, methanol, acetone, and diethyl ether). To this reddish solution was then added in 8 mL of CH_2Cl_2 a preparation of [Cu(CH_3CN)$_2$-(PPh_3)$_2$](BF_4), obtained from 95.6 mg (0.304 mmol) of [Cu(CH_3CN)$_4$]-(BF_4) and 159.3 mg (0.607 mmol) of PPh_3. The color of the solution turned deep red immediately. After 43 h all the copper powder had been used up and the volume of the solution was reduced to about one-fourth. Treatment with pentane produced a red oil that produced a red solid after addition of little dichloromethane and diethyl ether. Washing with pentane, drying in vacuo, dissolution in 8 mL of acetonitrile, filtration from insoluble material, and removal of the solvent gave analytically pure **1** as a very air- and moisture-sensitive red material in 57% yield (260 mg). Anal.Calcd for $C_{82}H_{66}BCu_2F_4N_8P_4$ (1501.28 g/mol): C, 65.60; H, 4.43; N, 7.46. Found: C, 64.89; H, 4.32; N, 7.47.

{(μ-H_2bmtz)[Cu(PPh_3)$_2$]$_2$}(BF_4)$_2$·CH_2Cl_2 (2·CH_2Cl_2). To 52.4 mg (0.167 mmol) of [Cu(CH_3CN)$_4$](BF_4) in 15 mL of dried dichloromethane was added 88.0 mg (0.336 mmol) of PPh_3 dissolved in 9 mL of CH_2Cl_2. After the mixture was stirred for 5 h at room temperature, a solution of 20.0 mg (0.083 mmol) of H_2bmtz[8] in 8 mL of CH_2Cl_2 was added and the orange solution was stirred for 16 h. Addition of pentane precipitated the product, which was recrystallized from dichloromethane/pentane to yield 100 mg (72%) of a bright-orange material with moderate air sensitivity. Anal. Calcd for $C_{83}H_{70}B_2Cl_2$-$Cu_2F_8N_8P_4$ (1674.95 g/mol): C, 59.52; H, 4.21; N, 6.69. Found: C, 59.58; H, 4.05; N, 6.69. ^{1}H NMR (CD_2Cl_2): δ = 8.80 (br, 4H, H$^{4,4',6,6'}$), 7.92 (br s, 2H, N^{1,4}−H), 7.76 (t, 2H, H$^{5,5'}$), 7.43−7.37, and 7.29−7.17 (m, 60H, phenyl-H); $^3J_{4,5} = {}^3J_{5,6}$ = 4.9 Hz.

Crystallography. Single crystals were obtained through slow evaporation of a saturated nitromethane solution (bmtz, dark-red rods, 0.5 mm × 0.2 mm × 0.2 mm) or through slow condensation of pentane into a solution of **1** or **2** in dichloromethane at 8 °C (**1**·2 CH_2Cl_2, dark-red rods, 0.6 mm × 0.2 mm × 0.2 mm) or 22 °C (**2**·CH_2Cl_2, orange platelets, 0.4 mm × 0.4 mm × 0.15 mm).

Siemens P3 and P4 diffractometers with Mo Kα radiation (λ = 0.710 73 Å) were used for data collection at 173 K. Intensity measurements were performed using ω scans. The structures were solved by direct methods with refinement by full-matrix least squares of F^2 using SHELXTL 5.1. Absorption correction was carried out via ψ scan for compound **2** only ($0.749 < T < 0.894$).

Crystallographic and refinement data are summarized in Table 1. All atoms of bmtz were refined using anisotropic temperature factors. For **1**·2 CH_2Cl_2 the hydrogen atoms of aromatic rings were refined freely; their isotropic temperature factors were set at those of the bound carbon atoms, multiplied by 1.2. The hydrogen atoms of the dichloromethane solvate molecules were introduced at ideal positions. The tetrafluoroborate anion was found disordered; two alternative positions with 67% and 33% weighting were used for the refinement. For **2**·CH_2Cl_2 all hydrogen atoms were introduced at ideal positions; their isotropic temperature factors were set at those of the bound carbon atoms, multiplied by 1.2. The CH_2Cl_2 solvate molecule was found disordered; two alternatives (each of 50% probability) with common chlorine positions were used in the refinement. One of the BF_4^- ions

(24) Bu, X.-H.; Morishita, H.; Tanaka, K.; Biradha, K.; Furusho, S.; Shionoya, M. *J. Chem. Soc., Chem. Commun.* **2000**, 971.
(25) Schwach, M.; Hausen, H.-D.; Kaim, W. *Inorg. Chem.* **1999**, *38*, 2242.
(26) Kaim, W.; Ernst, S.; Kohlmann, S.; Welkerling, P. *Chem. Phys. Lett.* **1985**, *118*, 431.
(27) Kaim, W.; Kohlmann, S. *Inorg. Chem.* **1986**, *25*, 3442.
(28) Klein, A.; McInnes, E. J. L.; Scheiring, T.; Zalis, S. *J. Chem. Soc., Faraday Trans.* **1998**, *94*, 2979.
(29) Doslik, N.; Sixt, T.; Kaim, W. *Angew. Chem.* **1998**, *110*, 2125; *Angew. Chem., Int. Ed.* **1998**, *37*, 7, 2403.

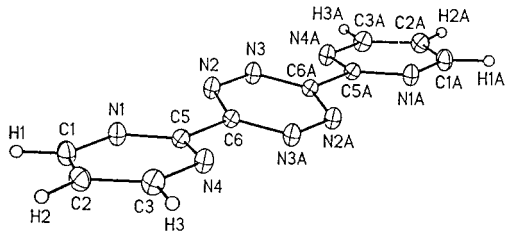

Figure 1. Molecular structure of bmtz in the crystal.

Table 2. Bond Lengths [Å] and Angles [deg] of bmtz[a]

N1−C5	1.3330(16)	C2−C3	1.380(2)
N1−C1	1.3436(17)	N3−C6A	1.3437(16)
C1−C2	1.382(2)	C3−N4	1.3412(17)
N2−N3	1.3296(15)	N4−C5	1.3351(17)
N2−C6	1.3393(17)	C5−C6	1.4930(16)
C5−N1−C1	115.49(12)	N1−C5−N4	127.25(12)
N1−C1−C2	122.50(13)	N1−C5−C6	117.04(11)
N3−N2−C6	117.26(11)	N4−C5−C6	115.71(11)
C3−C2−C1	116.66(12)	N2−C6−N3A	124.85(11)
N2−N3−C6A	117.90(11)	N2−C6−C5	118.01(11)
N4−C3−C2	122.52(13)	N3A−C6−C5	117.15(11)
C5−N4−C3	115.59(12)		

[a] Symmetry transformations used to generate equivalent atoms: (A) $-x, -y + 1, -z + 2$.

was also disordered; refinement was performed with two alternative positions with 56.4% and 43.6% weighting factor.

Results and Discussion

Syntheses and Structures. The dark-red ligand bmtz as synthesized by the reaction of 2-cyanopyrimidine with hydrazine[8] could be crystallized from nitromethane for X-ray diffraction. Reaction of bmtz with 2 equiv of $[Cu(PPh_3)_4](BF_4)$ yielded a very labile species assumed to be $\{(\mu\text{-bmtz})[Cu(PPh_3)_2]_2\}^{2+}$; it disintegrates above 210 K. Facile dissociation from the weakly basic bmtz and enhanced reducibility through coordination are considered responsible for this lability.

Reaction of bmtz with Cu, PPh_3, and $[Cu(PPh_3)_2(CH_3CN)_2](BF_4)$ in dry CH_2Cl_2 under argon produced the air- and moisture-sensitive red radical complex $\{(\mu\text{-bmtz}^{\bullet-})[Cu(PPh_3)_2]_2\}(BF_4)$ (**1**), which was obtained in single crystal form as bis-dichloromethane solvate for X-ray diffraction from pentane/dichloromethane. The above route was chosen to avoid using hydrated $Cu(BF_4)_2$ in a comproportionation reaction,[25] which yields dihydro derivatives as unwanted side products. The higher sensitivity of **1** in comparison to the sensitivity of the bptz analogue[25] is attributed to the presence of additional nucleophilic N centers for protonation-assisted degradation processes.

The light-orange compound $\{(\mu\text{-}H_2\text{bmtz})[Cu(PPh_3)_2]_2\}(BF_4)_2$ (**2**) was obtained from $[Cu(PPh_3)_2(CH_3CN)_2](BF_4)$ and H_2-bmtz[8,11] in dichloromethane.

Crystallographic data of bmtz and of the compounds **1**·2 CH_2Cl_2 and **2**·CH_2Cl_2 are summarized in Table 1, and selected bond data are listed in Tables 2−4. Figures 1−5 illustrate the molecular structures of the bmtz-containing species.

The structure of the free ligand bmtz (Figure 1, Table 2) is not esssentially different from that of the related bptz.[28] Because of the replacement of the two remaining ortho CH groups in the outer rings by N, the dihedral angle between these rings and the central tetrazine decreases from 19.1° in bptz[28] to 12.5° in bmtz. Stacking of the aromatic systems in the crystal occurs; however, the closest interatomic contact at 3.05 Å between N3 and N3A of neighboring molecules lies in the region of the sum of the van der Waals radii.

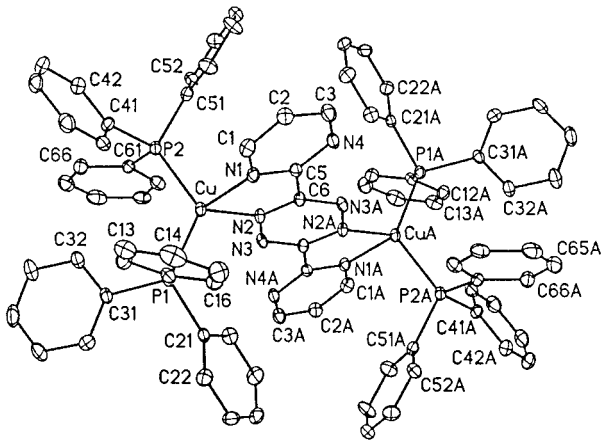

Figure 2. Molecular structure of $\{(\mu\text{-bmtz})[Cu(PPh_3)_2]_2\}^{\bullet+}$ in the crystal of **1**·$2CH_2Cl_2$.

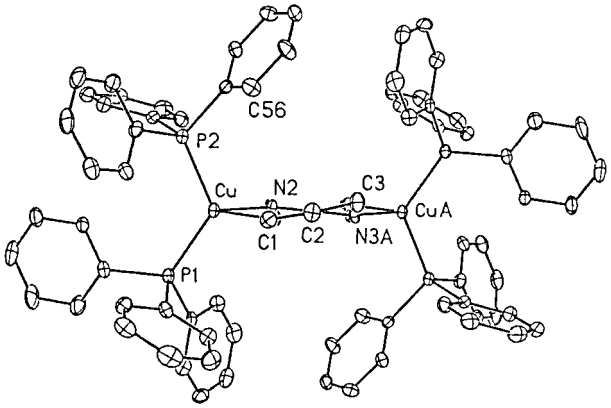

Figure 3. View of the structure of $\{(\mu\text{-bmtz})[Cu(PPh_3)_2]_2\}^{\bullet+}$ along the C2−C2A axis.

Table 3. Selected Distances [Å] in **1**·$2CH_2Cl_2$ and **2**·CH_2Cl_2[a]

	$\{(\mu\text{-bmtz})[Cu(PPh_3)_2]_2\}^{\bullet+}$		
Cu−N1	2.133(6)	N2−N3	1.380(7)
Cu−N2	1.994(5)	N3−C6A	1.321(8)
Cu−P1	2.225(2)	N4−C5	1.319(9)
Cu−P2	2.238(2)	N4−C3	1.322(9)
N1−C1	1.332(9)		
N1−C5	1.346(8)	Cu−CuA	6.680(2)
N2−C6	1.327(8)		
	$\{(\mu\text{-}H_2\text{bmtz})[Cu(PPh_3)_2]_2\}^{2+}$		
Cu1−N1	2.072(5)	N3−C10	1.376(8)
Cu1−N2	2.167(5)	N4−C3	1.335(9)
Cu1−P1	2.228(2)	N4−C4	1.335(8)
Cu1−P2	2.279(2)	N5−C9	1.345(8)
Cu2−N5	2.089(5)	N5−C8	1.347(9)
Cu2−N6	2.212(6)	N6−C10	1.275(8)
Cu2−P3	2.264(2)	N6−N7	1.420(7)
Cu2−P4	2.269(2)	N7−C5	1.396(8)
N1−C4	1.341(8)	N8−C9	1.327(8)
N1−C1	1.343(8)	N8−C6	1.333(10)
N2−C5	1.288(8)		
N2−N3	1.426(7)	Cu1−Cu2	7.116(3)

[a] Symmetry transformations used to generate equivalent atoms: (A) $-x + 1/2, -y + 1/2, -z + 2$.

The molecular structure of the dinuclear radical cation in **1**·2 CH_2Cl_2 (Figures 2 and 3, Table 3) shows some significant changes in the bridging ligand with regard to the bond lengths of the central tetrazine ligand (see below; Table 5). The orientation of the six-membered rings is only slightly altered relative to bmtz (Figure 3), and the dihedral angle is slightly increased from 12.5° to 16.6°. In comparison, the related $\{(\mu\text{-bptz})[Cu(PPh_3)_2]_2\}(BF_4)$ exhibits only a 5.8° interplanar angle.[25]

Table 4. Selected Bond Angles [deg] in **1**·2CH_2Cl_2 and **2**·CH_2Cl_2

	{(μ-bmtz)[Cu(PPh_3)$_2$]$_2$}$^{\bullet+}$		
N2−Cu−N1	78.8(2)	N2−Cu−P2	112.00(18)
N2−Cu−P1	115.53(18)	N1−Cu−P2	104.19(17)
N1−Cu−P1	113.50(17)	P1−Cu−P2	123.36(8)
	{(μ-H_2bmtz)[Cu(PPh_3)$_2$]$_2$}$^{2+}$		
N1−Cu1−N2	77.8(2)	N5−Cu2−N6	77.1(2)
N1−Cu1−P1	129.49(16)	N5−Cu2−P3	111.77(18)
N2−Cu1−P1	121.32(15)	N6−Cu2−P3	109.72(16)
N1−Cu1−P2	99.65(16)	N5−Cu2−P4	115.16(18)
N2−Cu1−P2	98.01(16)	N6−Cu2−P4	106.34(16)
P1−Cu1−P2	120.09(7)	P3−Cu2−P4	125.50(8)

Scheme 1

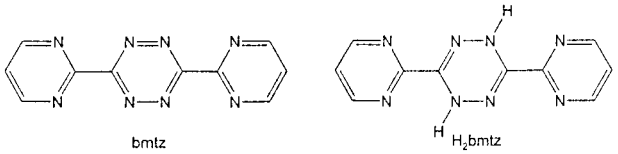

Scheme 2

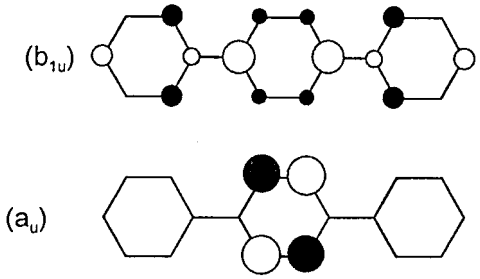

The twisted structure (Figure 3) results in a skewed arrangement at the metal centers where the P1−Cu−P2 plane makes an 80.3° angle with the tetrazine plane. The coordination geometry at the copper centers is distorted tetrahedral. Whereas the Cu−P distances are rather similar, the Cu−N distances vary much more significantly in **1**·2 CH_2Cl_2 (Δ = 0.139 Å) than in {(μ-bptz)[Cu(PPh_3)$_2$]$_2$}(BF_4) (Δ = 0.052 Å).[25] In both cases, the bonds to the tetrazine−N atoms are shorter than those to the pyridyl or pyrimidyl nitrogen centers. This general result is not unexpected because the spin and thus the added charge are concentrated in the tetrazine ring, as will be shown below; however, the strongly dissymmetric bonding of copper(I) to the nitrogen atoms of bmtz$^{\bullet-}$ in **1**·2 CH_2Cl_2 is remarkable. At 1.994(5) Å the Cu−N(tetrazine) bond is shorter even than that in related copper(I) complexes of azo ligands[30] and their anion radicals.[29,31] The weaker basicity of pyrimidine N vs pyridine N centers[14,16] is obviously not compensated by a better acceptor effect because the singly occupied molecular orbital (SOMO), a_u (Scheme 2), has vanishingly small contributions from the peripheral rings.[8,14]

As a consequence of the tighter binding to the tetrazine ring, the copper atoms in **1**·2 CH_2Cl_2 are separated by 6.680 Å in comparison to 6.743 Å for {(μ-bptz)[Cu(PPh_3)$_2$]$_2$}(BF_4).[25]

The crucial and expected[10,32] special feature in the structure of complex **2**·CH_2Cl_2 is the pronounced boat conformation of the 1,4-dihydro-1,2,4,5-tetrazine ring in coordinated H_2bmtz (Figures 4 and 5). The dihedral angle between planes intersecting at the sp^3 centers N3 and N7 (Figure 5) is 144.3°, compared with 148° of free 1,4-dihydro-1,2,4,5-tetrazine.[10] As in **1**·2 CH_2Cl_2, the pyrimidyl rings are twisted by about 15° relative to the corresponding planes of the central ring, and the copper(I) centers are distorted tetrahedral; in all instances (**1** and **2**), the sum of angles at the metal atoms lie around 646°, i.e., halfway between the values for an ideal tetrahedron (657°) and a trigonal pyramid (630°).

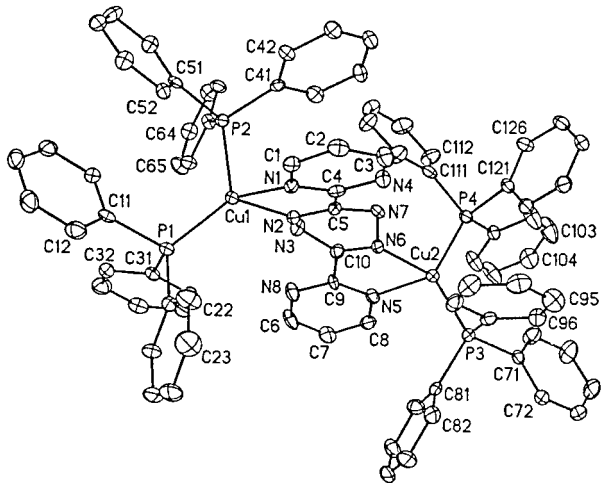

Figure 4. Molecular structure of {(μ-H_2bmtz)[Cu(PPh_3)$_2$]$_2$}$^{2+}$ in the crystal of **2**·CH_2Cl_2.

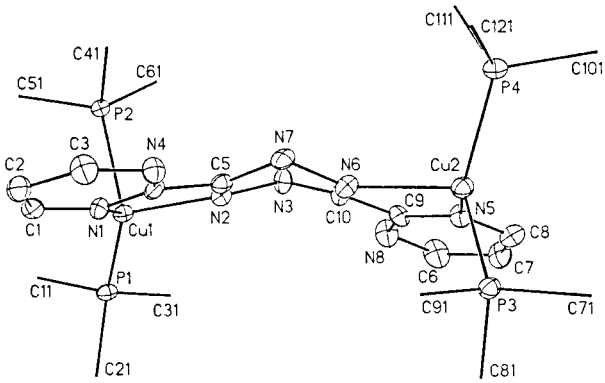

Figure 5. View of the structure of {(μ-H_2bmtz)[Cu(PPh_3)$_2$]$_2$}$^{2+}$ along the N3−N7 axis. Phenyl rings and H atoms at N3 and N7 are omitted for clarity.

The copper−nitrogen bonds are lengthened in **2**·CH_2Cl_2 relative to those of **1**·2 CH_2Cl_2, those to N(pyrimidine) by about 0.05 Å, and those to N(tetrazine) by about 0.2 Å. This result reflects the removal of negative charge by protonation. Neither Coulombic effects nor strong back-donation are now available for enhanced bonding to the bridging ligand; accordingly, compound **2** dissociates rapidly in acetonitrile. At 7.116 Å the Cu−Cu distance is appreciably lengthened relative to that in **1**·2 CH_2Cl_2 (6.680 Å). Intra- and intermolecular hydrogen bonding is insignificant because of intermolecular shielding by the PPh_3 ligands and unfavorable intramolecular orientation resulting in distances greater than 2.5 Å between H($N_{tetrazine}$) and neighboring $N_{pyrimidine}$, although the N4−N7 and N3−N8 distances lie at 2.73 Å. Unusually short contacts involving the phenyl rings could not be observed for either dicopper complex (Figures 3 and 5), which rules out the π/π interaction found in other dinuclear compounds between phenylphosphanecopper(I) fragments and N heterocycles.[25,33−35]

(30) Kaim, W.; Kohlmann, S.; Jordanov, J.; Fenske, D. *Z. Anorg. Allg. Chem.* **1991**, *598/599*, 217.
(31) Moscherosch, M.; Field, J. S.; Kaim, W.; Kohlmann, S.; Krejcik, M. *J. Chem. Soc., Dalton Trans.* **1993**, 211.
(32) Kaim, W. *Rev. Chem. Intermed.* **1987**, *8*, 247.
(33) Vogler, C.; Hausen, H.-D.; Kaim, W.; Kohlmann, S.; Kramer, H. E. A. Rieker, J. *Angew. Chem.* **1989**, *101*, 1734; *Angew. Chem., Int. Ed. Engl.* **1989**, *28*, 1659.

Scheme 3

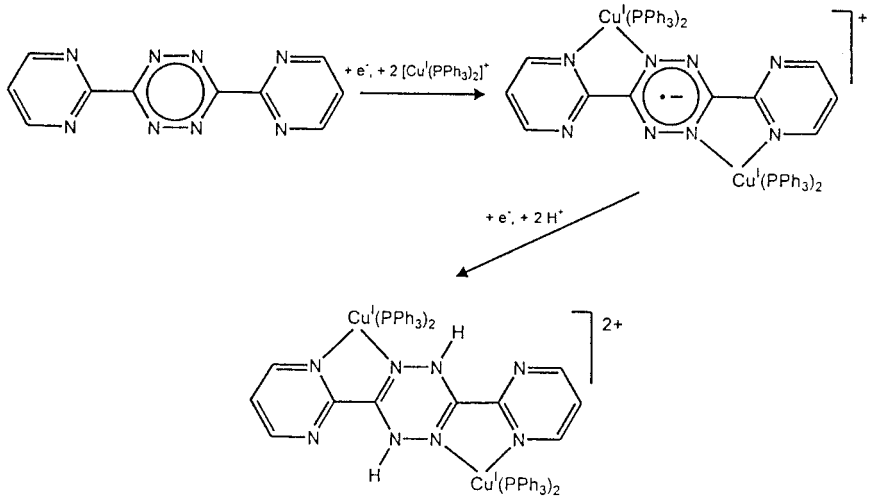

Table 5. Bond Lengths[a] in the Central Tetrazine Ring for Three Oxidation States of bmtz

compound	*d*(N−N)	*d*(C−NX)	*d*(C−NY)	X	Y
bmtz	1.330(2)	1.339(2)	1.344(2)	*b*	*b*
{(*μ*-bmtz)[Cu(PPh$_3$)$_2$]$_2$}$^{\bullet+}$ [c]	1.380(7)	1.321(8)	1.327(8)	*b*	Cu
{(*μ*−H$_2$bmtz)[Cu(PPh$_3$)$_2$]$_2$}$^{2+}$ [d]	1.426(7)	1.376(8)	1.288(8)	H	Cu
	1.420(7)	1.396(8)	1.275(8)		

[a] In Å. [b] Lone pair. [c] From **1**·2CH$_2$Cl$_2$. [d] From **2**·CH$_2$Cl$_2$.

Table 6. Electrochemical Data of Ligands and Complexes[a]

compound	$E_{1/2(ox)}$	$E_{1/2(red)}$	temp[b]	solvent[c]	ref
bmtz$^{\bullet-}$	−1.12	−2.17[d]	298	CH_3CN	8
H_2bmtz	0.28	−2.23[d]	298	CH_3CN	8, 11
1	−0.26[e]	−1.90[d]	203	CH_2Cl_2	this work
2	*e*	−1.39	203	CH_2Cl_2	this work
{(*μ*-bptz)[Cu(PPh$_3$)$_2$]$_2$}(BF$_4$)	−0.35[e]	−2.06[d]	298	CH_2Cl_2	25

[a] From cyclic voltammetry at 50 or 100 mV/s. Potentials *E* in V vs ferrocene/ferrocenium. [b] In K. [c] Electrolyte, 0.1 or 0.2 M Bu_4NPF_6. [d] Peak potential for irreversible process. [e] Further irreversible oxidation at about +0.9 V.

The bond lengths within the tetrazine ring vary quite systematically in the series bmtz, **1**·2CH$_2$Cl$_2$, and **2**·CH$_2$Cl$_2$, as outlined in Table 5. In agreement with changing bond orders as illustrated by the electron pair formulas (Scheme 3) the N−N bond lengthens continuously from bond order 1.5 to a single bond, and the corresponding C−NX bond, which gets protonated in H_2bmtz, exhibits a less pronounced behavior. As a countermove, the other C−N bond (C−NY in Table 5) shortens to an imine double bond, binding the metal. In contrast to the central tetrazine ring, the 2-pyrimidyl rings exhibit no significant structural changes in that series, which suggests that their system is not involved in the accommodation of the added electrons. This result parallels the observations made for the partially characterized bptz system, although the pyridine substituents there[25] have been replaced by the better accepting pyrimidine rings in bmtz. Spectroscopic studies, especially EPR hyperfine interaction, will confirm these structural results.

Cyclic Voltammetry. Considering the lability of {(*μ*-bmtz)[Cu(PPh$_3$)$_2$]$_2$}$^{2+}$ above 210 K, low-temperature measurements in dichloromethane solution were used for systems **1** and **2**. The data are summarized in Table 6. The radical complex **1** is reversibly oxidized at 203 K to {(*μ*-bmtz)[Cu(PPh$_3$)$_2$]$_2$}$^{2+}$ at a much less negative potential than the free bmtz$^{\bullet-}$ ligand (Table 6). This result illustrates the strong Coulombic effect by addition of two cationic metal centers to the site of electron addition. The reduction of **1** is totally irreversible at a very negative potential, confirming an extremely large stability range of about 1.6 V for the isolable radical complex intermediate. Such values corresponding to comproportionation constants $K_c > 10^{20}$ have similarly been observed for the corresponding bptz complex where the absolute potentials lie at more negative values.[25]

Surprisingly, complex **2** is also reversibly reducible at 203 K, although at a rather negative potential (Table 6). Free H_2-bmtz is only irreversibly reduced.[8] Both **1** and **2** exhibit irreversible oxidation processes at about +0.9 V vs ferrocene/ferrocenium, which are attributed to the oxidation of copper(I), PPh_3, and, for **2**, the H_2bmtz ligand.

Absorption Spectroscopy. The radical complex **1** exhibits long-wavelength absorptions at 510(sh) and 430 nm ($\epsilon = 6100$ M^{-1} cm^{-1}). They are assigned to metal-to-ligand charge transfer (MLCT) transitions from the filled d orbitals of the copper(I) centers (d^{10} configuration) to the still half-unoccupied π^* orbital (a_u) of bmtz. For the labile {(*μ*-bmtz)[Cu(PPh$_3$)$_2$]$_2$}$^{2+}$ the MLCT band occurs at much lower energy at 727 nm, in agreement with a more stabilized *empty* acceptor orbital on bmtz. Accordingly, the MLCT band is still further shifted to higher energies in complex **2**; the band lies at 400 nm ($\epsilon = 3100$ M^{-1} cm^{-1}). Because the tetrazine-centered a_u MO (Scheme 2) is now fully occupied, this transition must occur to the next unoccupied MO (b_{1u}), which has appreciable contributions from the pyrimidine rings. It is not surprising that corresponding dicopper(I) complexes bridged by 2,2′-bipyrimidine have similar absorption spectra,[33−35] confirming the nonparticipation of the dihydrotetrazine part of the bridging ligand of **2** in the creation of low-lying excited charge-transfer states.

EPR Spectroscopy (X and W Bands). The paramagnetic complex **1** exhibits partially resolved hyperfine structure in the X-band spectrum at ambient temperature. A tentative simulation involving ^{63,65}Cu ($I = {}^3/_2$), ^{31}P ($I = {}^1/_2$), and ^{14}N ($I = 1$) isotopes is shown in Figure 6, and the data are summarized in Table 7. Continuous wave electron nuclear double resonance (CW-ENDOR) was not possible because the ESR transition could not be saturated; a differentiation between the ^{63}Cu and ^{65}Cu isotopes[34,36] could not be observed because of the unfavorable ratio of the line width to copper coupling constant.

(34) Vogler, C.; Kaim, W.; Hausen, H.-D. *Z. Naturforsch.* **1993**, *48b*, 1470.
(35) Schwach, M.; Hausen, H.-D.; Kaim, W. *Chem.—Eur. J.* **1996**, *2*, 446.
(36) Kaim, W.; Moscherosch, M. *J. Chem. Soc., Faraday Trans.* **1991**, *87*, 3185.

Table 7. EPR Data of Paramagnetic Species[a]

compound	$a_N/a_{N'}$[b]	$a(^{65}Cu/^{63}Cu)$	a_p	g_{iso}	solvent	ref
$bmtz^{\bullet-}$ [c]	_/0.52			2.0040	THF	8
1[d]	0.609/0.486	0.824/0.769	0.769	2.0053[e]	CH_3CN	this work
$\mathbf{2}^{\bullet-}$ [f]	*f*	*f*	*f*	2.0033	CH_2Cl_2	this work
$\{(\mu\text{-bptz})[Cu(PPh_3)_2]_2\}^{\bullet+}$ [g]	0.605/0.463	0.758 [g]	0.910	2.0055[h]	CH_2Cl_2	37, 40
$\{(\mu\text{-bpym})[Cu(PPh_3)_2]_2\}^{\bullet+}$ [c]	0.215/_	0.691/0.646	0.691	2.0032	CH_2Cl_2	34

[a] Coupling constants *a* in mT. X-band data unless stated otherwise. [b] Coordinated (N) and uncoordinated (N′) nitrogen atoms of the tetrazine ring. [c] At 298 K. [d] At 273 K, copper isotope coupling unresolved (values from computer simulation). [e] W-band data at 20 K (powder): $g_1 = g_2 = 2.0062$, $g_3 = 2.0021$. [f] At 200 K, hyperfine coupling not resolved. [g] At 300 K, no differentiation between the copper isotopes. [h] 245 GHz data at 4 K in frozen acetone/ethanol (5/1) solution: $g_1 = g_2 = 2.0067$, $g_3 = 2.0026$.

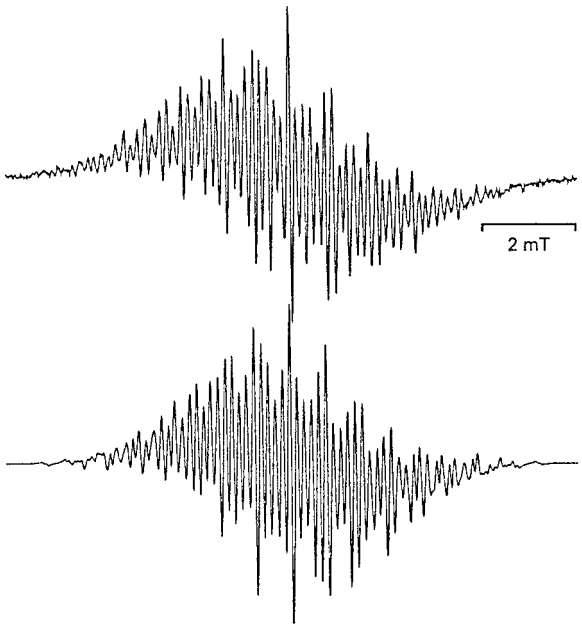

Figure 6. X-band EPR spectrum of **1** in acetonitrile at 273 K (top) and graphical simulation with the data from Table 7 (bottom).

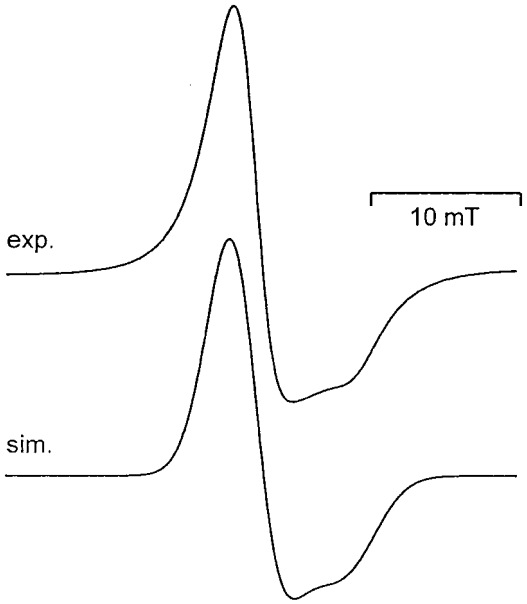

Figure 7. W-band EPR spectrum of **1** (powder) at 20 K (top) and graphical simulation with the data from Table 7 (bottom).

The coupling constants are comparable[37] to those of $\{(\mu\text{-bptz})[Cu(PPh_3)_2]_2\}^{\bullet+}$ (Table 7), confirming the spin localization at the two different kinds of nitrogen atoms in the tetrazine ring with secondary spin transfer to the coordinated metal centers and their additionally bound donor atoms (^{31}P). A π/σ hyperconjugation mechanism has been invoked for this spin transfer,[34] and the conformational sensitivity of this mechanism may explain the difference in $a(^{31}P)$ between $bmtz^{\bullet-}$ and $bptz^{\bullet-}$ compounds (Table 7). The slightly larger copper coupling constants for **1** are in agreement with the structurally confirmed stronger $Cu-N_{tetrazine}$ bonding.

The coupling constants of $^{63,65}Cu$ and ^{31}P are rather small when compared with typical values of $a(^{63.65}Cu) \approx 8$ mT for copper(II) species[38] or with the isotropic hyperfine constants $a_o = 213.92$ mT (^{63}Cu), 228.92 mT (^{65}Cu), and 474.79 mT (^{31}P).[39] The hyperfine results thus confirm the predominantly ligand-centered spin in complex **1**.

Additional evidence comes from the isotropic *g* value of 2.0053, which lies close to that of free $bmtz^{\bullet-}$ (2.0040).[8] The absence of any *g* component features in the low-temperature (120 K) X-band spectrum of **1** due to unresolved overlap from hyperfine lines prompted a study at W-band frequency (94 GHz). High-field EPR has proven valuable for determining the *g* anisotropy of copper(I)-containing radical complexes.[40] The W-band spectrum of **1** at 20 K (Figure 7) exhibits an axial symmetry with *g* components similar to those determined by 245 GHz EPR for $\{(\mu\text{-bptz})[Cu(PPh_3)_2]_2\}(BF_4)$.[40] The axial splitting stands in contrast to the rhombic splitting observed for related dicopper(I) complexes bridged by azo-containing anion radical ligands.[40] We attribute this effect to the unique localization of spin at the tetrazine ring.

Compound **2** could be reversibly reduced only at low temperatures (Table 6). In fluid solution at 200 K and in the glassy frozen state at 117 K, $\mathbf{2}^{\bullet-}$ gave only an unresolved EPR line of about 10 mT total width. The isotropic *g* value of 2.0033 points to a predominantly ligand-centered spin with more C than N participation, in agreement with the occupation of the b_{1u} MO by the unpaired electron. The numerous additional hyperfine coupling from ^1H and ^{14}N centers of the pyrimidine rings would explain the absence of resolution due to numerous overlapping hyperfine lines.

Although the series of crystallographically and spectroscopically characterized compounds in Scheme 3 does not constitute a simple redox triad, i.e., two consecutive redox pairs,[41] they

(37) Kaim, W.; Kohlmann, S. *Inorg. Chem.* **1987**, *26*, 1469.
(38) Weil, J. A.; Bolton, J. R.; Wertz, J. E. *Electron Paramagnetic Resonance*; Wiley: New York, 1994.
(39) Goodman, B. A.; Raynor, J. B. *Adv. Inorg. Chem. Radiochem.* **1970**, *13*, 135.
(40) Barra, A.-L.; Brunel, L.-C.; Baumann, F.; Schwach, M.; Moscherosch, M.; Kaim, W. *J. Chem. Soc., Dalton Trans.* **1999**, 3855.
(41) (a) Boyd, D. C.; Connelly, N. G.; Garcia Herbosa, G.; Hill, M. G.; Mann, K. R.; Mealli, C.; Orpen, A. G.; Richardson, K. E.; Rieger, P. H. *Inorg. Chem.* **1994**, *33*, 960. (b) Bartlett, I. M.; Carlton, S.; Connelly, N. G.; Harding, D. J.; Hayward, O. D.; Orpen, A. G.; Ray, C. D.; Rieger, P. H. *J. Chem. Soc., Chem. Commun.* **1999**, 2403. (c) Baik, M.-H.; Ziegler, T.; Schauer, C. K. *J. Am. Chem. Soc.* **2000**, *122*, 9143.

illustrate how chemical reactivity and structure are connected with electron transfer. The lability of both the ligand-oxidized $\{(\mu\text{-bmtz})[Cu(PPh_3)_2]_2\}^{2+}$ and the 1,4-dihydro form (**2**) of the dicopper(I) system contrasts with the dissociative stability of the radical intermediate **1**, which, despite sensitivity toward protons, oxygen, and other electrophiles in solution, can be viewed as an interesting new kind of paramagnetic component in solids. For instance, several metal complexes with the tetrazine-containing verdazyl radical function have been described very recently.[42−44]

Acknowledgment. Support from Deutsche Forschungsgemeinschaft, Volkswagenstiftung, and Fonds der Chemischen Industrie is gratefully acknowledged. We thank in particular Graduiertenkolleg "Magnetische Resonanz" for its support.

Supporting Information Available: Details of the X-ray structure determinations in CIF format. This material is available free of charge via the Internet at http://pubs.acs.org.

IC001228Q

(42) Brook, D. J. R.; Fornell, S.; Stevens, J. E.; Noll, B.; Koch, T. H.; Eisfeld, W. *Inorg. Chem.* **2000**, *39*, 562.

(43) Brook, D. J. R.; Fornell, S.; Noll, B.; Yee, G. T.; Koch, T. H. *J. Chem. Soc., Dalton Trans.* **2000**, 2019.

(44) Hicks, R. G.; Lemaire, M. T.; Thompson, L. K.; Barclay, T. M. *J. Am. Chem. Soc.* **2000**, *122*, 8077.